EXPERIMENTAL STUDIES OF ELECTROKINETIC CONVERSIONS IN A FLUID-SATURATED POROUS MEDIUM

Zhenya Zhu and M.Nafi Toksöz

Earth Resources Laboratory
Department of Earth, Atmospheric, and Planetary Sciences
Massachusetts Institute of Technology
Cambridge, MA 02139

ABSTRACT

The electrokinetic effect in a fluid-saturated porous rock is defined as the coupling and conversion between seismic and electric energies. When seismic waves propagate through a fluid-saturated formation and cause a pore fluid-flow relative to the solid matrix, the motion of the cations in the fluid- flow forms a streaming electrical current and induces an electromagnetic wave at any discontinuous interface of the formation or stationary electric potential inside the homogeneous formation. Another conversion of energies opposite to the seismoelectric conversion is when an alternating electric field induces a relative fluid-flow in a fluid-saturated porous rock where fluid-flow can generate an electroseismic wave in the rock. In this paper we study the electrokinetics in porous sandstone and man-made porous models at high frequencies. A P-wave or S-wave transducer excites different acoustic wave modes in a cylinder, layer, or borehole model. Our experiments observe and record the radial or stationary seismoelectric signals induced at the interface or inside the formation. Some relative experiments have confirmed the reliability of the electrokinetic phenomenon observed in our experiments and the mechanism that is different from the piezoelectric effect. The results show that the seismoelectric signal induced by the extensional or flexural wave in the sandstone cylinder is a stationary local electric potential. The seismoelectric signal induced at the interface of the layer model is an electromagnetic wave which can be received within the fluid-filled porous medium. Experimental measurements performed in a borehole model by means of vertical seismic profiling (VSP) and single borehole logging show it is possible to conduct seismoelectric measurements in a deep borehole of petroleum formation. Measurements of electrokinetics can thus provide an effective means for estimating parameters in a fluid-saturated porous formation.

Zhu and Toksöz

INTRODUCTION

The electrokinetic phenomenon in porous media is intimately related to the electro-chemistry of the interface region between a solid and a fluid. When a fluid electrolyte comes into contact with a neutral solid surface (like a quartz wall), anions from the electrolyte are chemically adsorbed to the surface. An excess of cations is left behind the negative layer and distributed near the surface. Some are bound so strongly that they are immobilized. Beyond this layer there are mobile cations (Pride and Morgan, 1991). When a fluid electrolyte moves related to a solid, the movement of the mobile cation forms an electric field. The potential associated with this electric field is called the streaming potential. In contrast, when an electric field drives a cation motion, the generated relative movement between the fluid and solid excites mechanic movement or an acoustic wave in a porous medium. Many laboratory experiments (Broz and Epstein, 1976; Ishido and Mizutani, 1981; Kuin and Stein, 1987; Cerda and Kiry, 1989; and Morgan et al., 1989) were performed to investigate the streaming potential generated by the flowing of different fluids at different pressures through porous sands or man-made porous material. In these experiments the electrolyte moves forward a certain direction or moves back and forth at low frequency range (usually under 1000 Hz).

The electrokinetic phenomenon of the conversion between seismic and electromagnetic energies was discovered and proposed to be used as an exploratory tool in the 1930s (Thompson, 1936; Belluigi, 1937). When seismic waves propagate through a fluid-saturated formation, the vibration and displacement of the grain and the pore fluid cause their relative motion. The mobile cations in the fluid act as a current source and induce an electric field in the formation. The current flows generate electromagnetic waves at the interface where the electric or acoustic properties are different on both sides. On the other hand, when the pore fluid with cations has a relative motion enforced by an alternating electric field, the relative action between the grain and pore fluid generates seismic waves. Theoretical studies have demonstrated electrokinetic effects in porous media (Kozak and Davis, 1987; Neev and Yeatts, 1989; Thompson and Gist, 1991; Pride and Morgan, 1991; Pride et al., 1993; Haartsen, 1995). Field tests have also observed seismoelectric effects (Martner and Sparks, 1959; Sobolev et al., 1984; Russell and Barker, 1991; Thompson and Gist, 1993). Because of the low signal-to-noise ratio in field tests, intensive data processing is needed to extract the electric signals; it is difficult to compare the field results to the theoretical calculations.

To investigate electrokinetic behavior and compare it with theoretical predictions, we studied the electrokinetic effect of a fluid-saturated sandstone or man-made porous medium in the M.I.T. Earth Resources Laboratory's ultrasonic laboratory, observed the seismoelectric and electroseismic conversions, and studied their characteristics and radiation. We constructed cylinder, layer, and borehole models to excite different acoustic wave modes. The seismoelectric potentials generated by the acoustic waves were measured with an electrode and compared with the acoustic waveforms. Relative experiments have eliminated the nonreliability in our experiments and confirmed the basic

principle that fluid-flow induces the seismoelectric effect.

EXPERIMENTS IN A CYLINDER MODEL

To excite a simple and pure acoustic mode, a cylinder model was made of Berea sandstone or Coconino sandstone 1.24 cm in diameter and 10 cm in length. Table 1 lists the properties of the sandstones. Figure 1 shows a diagram of the experimental setup. A water-saturated cylinder sample is placed between the acoustic source and receiver transducers. The measurement points of 0.2 cm in diameter and 1 cm in spacing are made of conducting glue on the sample surface along its axis. An electrode with a sharp pin-head touches these points consecutively and receives the electric potentials on the surface. The electric signals received through an amplifier and a filter are digitly recorded. A metal film shields the whole sample to prevent outside electric influence. If the source is a compressional wave transducer, an extensional wave is excited in the cylinder sample; if it is a shear transducer, a flexural wave can be excited. The electric pulse for exciting the acoustic transducer is a square wave with a high voltage of 500 volts. The width of the pulse is variable and is usually equal to the half cycle of the acoustic wave.

Figure 2 shows the seismoelectric signals generated by an acoustic compressional wave in the water-saturated Berea sandstone cylinder. The top trace (dashed line) in the plot is the acoustic wave received by the compressional transducer on the other end of the cylinder. The center frequency of these waveforms is approximately 18 kHz. The phase velocity determined by the slope of the waveforms is about 1700 m/s.

From the traveltime of the first arrivals, we know that the signals are not due to electric interference. Comparing these signals with the acoustic waveform received on the other end of the sample, we can see that the shape and the arrival time of the acoustic wave coincide with those of the electric signals. This means that the electric signals are generated by the extensional wave propagating along the cylinder sample.

A shear source transducer can excite a flexural wave in a cylinder model shown in Figure 1. Figure 3 shows electric signals generated by an acoustic shear wave and received by an electrode on the surface of the Coconino cylinder sample. The center frequency and the phase velocity of the signals recorded in Figure 3 are 27 kHz and about 1150 m/s, respectively. Despite the different orientations in particle motions of the extensional and flexural waves, once the relative motion between the pore fluid and the solid matrix is excited, both modes of the waves can generate seismoelectric signals in a fluid-saturated porous sandstone.

The received electric signals are related only to the acoustic wave arriving at the measurement point. In other words, the seismoelectric signals cannot be received at other points that are not disturbed by the acoustic wave, although the water-saturated sandstone cylinder is not an electric isolator. This means that the received electric signal is a stationary, local potential, which cannot propagate at electromagnetic speed within the sandstone cylinder. Basic principles of seismokinetics explain the reason: an

acoustic wave excites the charge motion in the pore fluid and induces the streaming potential in the disturbed area. If the porous rock is homogeneous, the sum of the streaming currents within the disturbed area should be equal to zero; therefore, they do not induce any electric potential outside the area. If the rock is mechanically or electrically nonhomogeneous (e.g., there is an interface with mechanical or electrical difference) the nonsymmetric streaming current will induce an electromagnetic wave which propagates at high speed and can be received anywhere. We made a layer rock model to investigate the electrokinetics at an interface.

The relationship between the acoustic wave and the seismoelectric signal and the effect of the conductivity of the saturant on the seismoelectric signal have been investigated experimentally using the measurement setup shown in Figure 1. We have also studied the opposite energy conversion from electric into acoustic energy (Zhu *et al.*, 1994).

EXPERIMENTS IN A LAYER MODEL

Layer models are made of natural sandstones or a man-made porous medium to investigate the seismoelectric field generated at an interface and within the porous medium.

Sandstone-Layer Model

The layer model is composed of a Lucite block and a piece of a sandstone rock (Figure 4). A compressional transducer, as an acoustic source, excites the P-wave which radiates at 45 degrees on the interface between the Lucite and the sandstone block. The center frequency of the acoustic wave is about 100 kHz. The Lucite block serves to delay the arrival time of the acoustic wave on the interface and eliminates the electric interference of the exciting pulse (500 V) on the seismoelectric signals. On the interface between the Lucite and the rock ten measurement points on 2 cm centers are made of conducting glue to measure the electric field. The rock sample is water-saturated Berea or Coconino sandstone. There is no air bubble entrapped at the interface and all of the possible gaps between the Lucite and the sandstone are saturated with water. The instrumentation of the system is depicted in Figure 1.

Measurements begin with the acquisition of acoustic waves by a small standard P-wave transducer at each measurement point on the Lucite. Figure 5 shows the received acoustic waveforms which are normalized by their maximum amplitude. Figures 6 and 7 show the electric signals which are generated by the acoustic wave and received by the electrode connecting the measurement points on the interface between the Lucite block and Berea or Coconino sandstone. The amplitude in Figure 5 and the following plots is normalized by the maximum of the amplitudes in each plot. Comparing these signals with the acoustic waveforms shown in Figure 5, we see that the arrival times, the shape of the waveforms, and the amplitude variation of the electric signals are in good agreement with the acoustic waves. Therefore, we conclude that the electric signals are indeed the seismoelectric ones generated on the interface between the nonpermeable

Lucite and water-saturated sandstone; the conversion between the acoustic and electric energies occurs here.

Man-Made Layer Model

In order to investigate the electrokinetics inside a homogeneous porous medium and to compare them with those at an interface, we made a layer model with a Lucite block and sand. The sand is glued with epoxy and poured onto the surface of the Lucite block. The physical properties are shown in Table 1. Four sets of electrodes made of fine wires are buried on the interface and in the glued sand with a spacing of 1 cm (Figure 8). The conductivity and permeability of the water-saturated glued sand are 280 $\Omega \cdot m$ and about 200 darcy, respectively. A P-wave transducer, as a source, is placed at the middle of the model.

Figure 9 shows the acoustic waveforms received by a small P-wave transducer on the Lucite bottom surface. The first arrivals in the waveforms are the compressional waves and the secondary arrivals are those reflected from the boundaries of the Lucite block. Figure 10 shows the waveforms of the electric signals received by electrode sets I, II, III, and IV. The arrival times and the amplitude variation of the electric signals shown in Figure 10a are in good agreement with the acoustic waves shown in Figure 9. This means the acoustic wave induces seismoelectric signals at the interface. From Figure 10b we see that the acoustic wave passing through the interface induces the seismoelectric signals inside the glued sand, and some electric signals at higher frequency and with lower amplitude are received before the acoustic wave reaches electrode set II. Comparing these waveforms with the first arrival of the electric signals in Figure 10a, we confirm that the first arrivals of the electric signals in Figure 10b are generated at the interface, then propagated in the medium with the electromagnetic wave velocity and finally received by electrode set II. Because the electromagnetic velocity is much faster than the acoustic velocity, there is virtually no time delay between the first arrivals of the signals shown in Figures 10a and 10b. In the signals received by electrode sets III and IV (Figures 10c and 10d), we can also observe the electric signals which are generated at the interface and then propagated into the glued sand.

Figure 11 shows the electric signals received by four electrodes at the same horizontal but different vertical locations. The distance of the electrodes from the interface is 0 cm, 1 cm, 2 cm and 3 cm, respectively. From these waveforms we see that there are two sets of the electric signals. One set is the first arrivals with the same arrival time. The other one is related to the acoustic wave propagating in the medium. This means that only the seismoelectric signal generated at the interface can be received by the other electrodes inside the homogeneous medium. The electric signal induced inside the medium cannot be received by the electrodes outside the area disturbed by the acoustic wave. We conclude that the seismoelectric signal generated at the interface is an electromagnetic wave. The experiment results have been compared with the theoretical calculation (Haartsen et al., 1995).

EXPERIMENTS IN A BOREHOLE MODEL

Due to the low efficiency of the seismoelectric conversion, the field measurement is only applied in exploring the shallow formation. To investigate the possibility of the direct seismoelectric measurement in a fluid-filled borehole, we made a borehole model (Figure 12) by pouring glued sand onto one side of a Lucite cylinder with a borehole along its axis and burying wire electrodes inside the sand. We have measured seismoelectric signals on the borehole wall and inside the porous medium by means of two methods similar to the VSP and single borehole logging, respectively. The acoustic sources are located on the side of the cylinder model and in the water-filled borehole, respectively.

Figure 13 shows a diagram of VSP measurement. A compressional wave transducer moves around the borehole on the side of the model. When a high voltage pulse excites the transducer and generates an acoustic wave in the model, we record the electric signals received by the electrodes on the borehole wall with the transducer movement of 30°/trace (Figure 14). Figure 15 shows the electric signals received by the electrodes at the same azimuth and different depth when the acoustic source is fixed at a certain position (180°). The acoustic wave induces a stronger seismoelectric (electromagnetic) wave (Figure 14a) at the interface between the Lucite and the porous medium, which propagates at the velocity of an electromagnetic wave in the medium and is received by the electrodes at a different depth of the borehole (Figures 14b-c). This method is useful for determining the formation interface by directly measuring the seismoelectric signals on the borehole wall. The signal-to-noise ratio of the recorded signals increases due to the direct measurement on the wall.

Figure 16 shows a diagram for measurements in a single water-filled borehole. Figure 17 shows the acoustic waves measured by an acoustic receiver in the borehole section of the porous medium when the acoustic source moves up in the Lucite section of the borehole. At the same time the electrodes on the borehole wall at different depths record the seismoelectric signals (Figure 18). It is clear that there are two kinds of seismoelectric signals induced by the P- and Stoneley wave in Figure 18. In this case, the electromagnetic wave induced at the interface between the Lucite and the porous medium is very weak because the main energy of the acoustic wave is concentrated in the borehole. The received seismoelectric wave is mainly the local electric potential. We may apply this method to measure seismoelectric signals in a deep petroleum formation. Because the acoustic source is close to the electrodes, it is possible to measure the borehole formation with higher resolution.

Relative Experiments

We have performed some relative experiments to confirm the seismoelectric phenomena observed in the previous experiments and to rule out the possibility of experimental errors. The measurement with a dry sandstone sample is performed using the setup shown in Figure 1. In other experiments with a layer model we have checked to see if the seismoelectric signals can be generated on the interface between the Lucite and air,

water, dry rock or unsolid sand, respectively.

The piezoelectric effect is a special phenomenon that needs to be distinguished from electrokinetics. The quartz grain in a sandstone is a piezoelectric crystal. When quartz is strained, an electric potential of a dipole moment is induced along its electric axis. The direction of the piezoelectric field depends on the orientation of the quartz grain which is random in sandstone. Therefore, when an acoustic wave propagates along a certain direction, both the amplitude and the polarization of the piezoelectric field generated by the acoustic wave depend on the orientations of the quartz grains.

Figure 19 shows the electric signals generated by a P-wave transducer and received on a dry Berea sandstone cylinder sample (Figure 1) that has been heated in a vacuum vessel for eight hours. From the time delay of the first arrivals in the signals we know that these electric signals are generated by the acoustic wave. On the other hand, not only the amplitude but also the phases of the first arrivals vary randomly with the measurement points. The maximum amplitude is about 20 μ V and much less than that of the seismoelectric signals (Figure 2). Therefore, we conclude that the electric potentials generated by the acoustic wave in a dry rock sample are due to the piezoelectric phenomenon. In contrast to the piezoelectric case, the electric fields generated by the same acoustic wave in a water-saturated rock sample are all in the direction of the pressure gradient (see Figure 2) because seismokinetic coupling depends on the fluid flow and is significantly different from piezoelectric coupling.

A Lucite block is used in the layer models to eliminate the interference of the source pulse (Figure 4). We have checked the electric field generated by the P-wave on the Lucite surface. No electric signal can be received on the interface between the Lucite and the air or water (free surface) at the same experimental scale as that in Figure 6. We also measured the electric fields on the interfaces where the Lucite block contacts dry Berea sandstone or water-saturated unconsolidated sand. In all of these cases, we cannot receive any electric signal at the same recording scale. The baseline experimental results confirm that the electrokinetics predicted and observed are quite separate from the piezoelectric effect in a crystal. The experiment with the unsolided sand shows that the electrokinetics depends on the relative fluid flow. Because in this case the sand is not consolidated and moves together with the fluid under acoustic pressure gradient, the relative motion between the fluid and the sand decreases and the amplitude of the seismoelectric signals is small.

CONCLUSIONS

Our experiments demonstrate seismoelectric conversion at a high frequency region in a fluid-saturated porous medium. The experimental results confirm that the mechanism of electrokinetics is different from that of piezoelectrics in a crystal. The electrokinetic phenomenon is closely related to the relative flow of the pore fluid to the solid matrix. The seismic waves with various modes, such as compressional, shear, extensional, flexural, and Stoneley waves, can generate seismoelectric signals in a fluid-saturated porous

formation.

The mechanism of the seismoelectric signals generated at an interface or inside a porous medium is the same, but there are two kinds of streaming potential—an electromagnetic wave that can propagate in the medium, and a stationary local potential. If there is a mechanic or an electric discontinuity in the porous medium (interface), the acoustic wave will induce an electromagnetic wave due to streaming current imbalances at the interface. The seismoelectric signal induced inside a homogeneous formation or on a free surface is a stationary local streaming potential, which can be measured by an electrode, but does not propagate within the medium nor can it be measured in an undisturbed area. The experiments with the borehole model investigate the possibility of seismoelectric measurement which is similar to vertical seismic profiling or acoustic well logging. Therefore, it would be a very useful means for exploring a fluid-saturated porous formation in geophysical prospecting.

The results of the experiment with complex models (layer and borehole models) only demonstrate the seismoelectric phenomena qualitatively. In future work, we will study the quantitative relationship between the seismoelectric signal and the formation parameters.

ACKNOWLEDGMENTS

REFERENCES

Belluigi, A., 1937, Seismic-electric prospecting, *The Oil Weekly*, 38–42.

Broz, Z., and N. Epstein, 1976, Electrokinetic flow through porous media composed of fine cylindrical capillaries, *J. Colloid and Interface Science, 56*, 605–612.

Cerda, C.M., and N.C. Kiry, 1989, The use of sinusoidal streaming flow measurements to determine the electrokinetic properties of porous media, *Colloids and Surfaces, 35*, 7–15.

Haartsen, M.W., 1995, Coupled electromagnetic and acoustic wavefield modeling in poro-elastic media and its applications in geophysical exploration, Ph.D. thesis, MIT.

Haartsen, M.W., Z.Zhu, and M.N. Toksöz, 1995, Seismoelectric experimental data and modeling in porous layer models at ultrasonic frequencies, SEG 65th Annual International Meeting Expanded Abstracts, PP5.10, 696–699, Houston, Texas.

Ishido, T., and H. Mizutani, 1981, Experimental and theoretical basis of electrokinetic phenomena in rock-water system and its applications to geophysics, *J. Geophys. Res., 86*, 1763–1775.

Kozak, M.W., and E.J. Davis, 1989, Electrokinetics of concentrated suspensions and porous media, *J. Colloid and Interface Science, 127*, 497–510, and *129*, 166–174.

Kuin, A.J., and H.N. Stein, 1987, Development of a new pore model: II Electrokinetic transport properties, surface conductance, and convective charge transport, *J. Colloid and Interface Science, 115*, 188–198.

Martner, S.T., and N.R. Sparks, 1959, The electroseismic effect, *Geophysics, 24*, 297–308.

Morgan, F.D., E.R. Williams, and T.R. Madden, 1989, Streaming potential properties of westerly granite with applications, *J. Geophys. Res., 94*, 12.449–12.461.

Neev, J., and F.R. Yeatts, 1989, Electrokinetic effects in fluid-saturated poroelastic media, *Physical Review B, 40*, 9135–9142.

Pride, S.R., and F.D. Morgan, 1991, Electrokinetic dissipation induced by seismic wave, *Geophysics, 56*, 914–925.

Pride, S.R., F.D. Morgan, and A.F. Gangi, 1993, Drag force of porous-medium acoustics, *Physical Review B, 47*, 4964–4978.

Russell, R.D. and A.S. Barker, Jr., 1991, Seismo-electric exploration: Expected signal amplitudes, *Geophysical Prospecting, 39*, 105–118.

Sobolev, G.A., V.M. Demin, B.B. Narod, and P. Whaite, 1984, Tests of piezo-electric and pulsed-radio methods for quartz vein and base-metal sulfides prospecting at Giant Yellowknife Mine, N.W.T., and Sullivan Mine, Kimberley, Canada, *Geophysics, 49*, 2178–2185.

Thompson, R.R., 1936, The seismic electric effect, *Geophysics, 1*, 327–335.

Thompson, A.H., and G.A. Gist, 1991, Electroseismic prospecting: SEG 61st Annual International Meeting Expanded Abstracts, Paper EM2.1, 425–427.

Thompson, A.H., and G.A. Gist, 1993 Geophysical applications of electrokinetic conversion, *The Leading Edge, 12*, 1169–1173.

Zhu, Z., C.H. Cheng, and M.N. Toksöz, 1994, Electrokinetic conversion in a fluid-saturated porous rock sample, SEG 64st Annual International Meeting Expanded Abstracts, Paper SL1.1, 425–427.

Table 1: Physical Parameters of Water-Saturated Samples

Sample	Density (g/cm^3)	Porosity (%)	Vp (m/s)	Vs (m/s)
Berea Sandstone	2.08	18.9	3050	1950
Coconino Sandstone	2.29	13.2	3680	2290
Glued Sand	1.71	25.6	2540	1200
Lucite	1.18	0.0	2700	1290
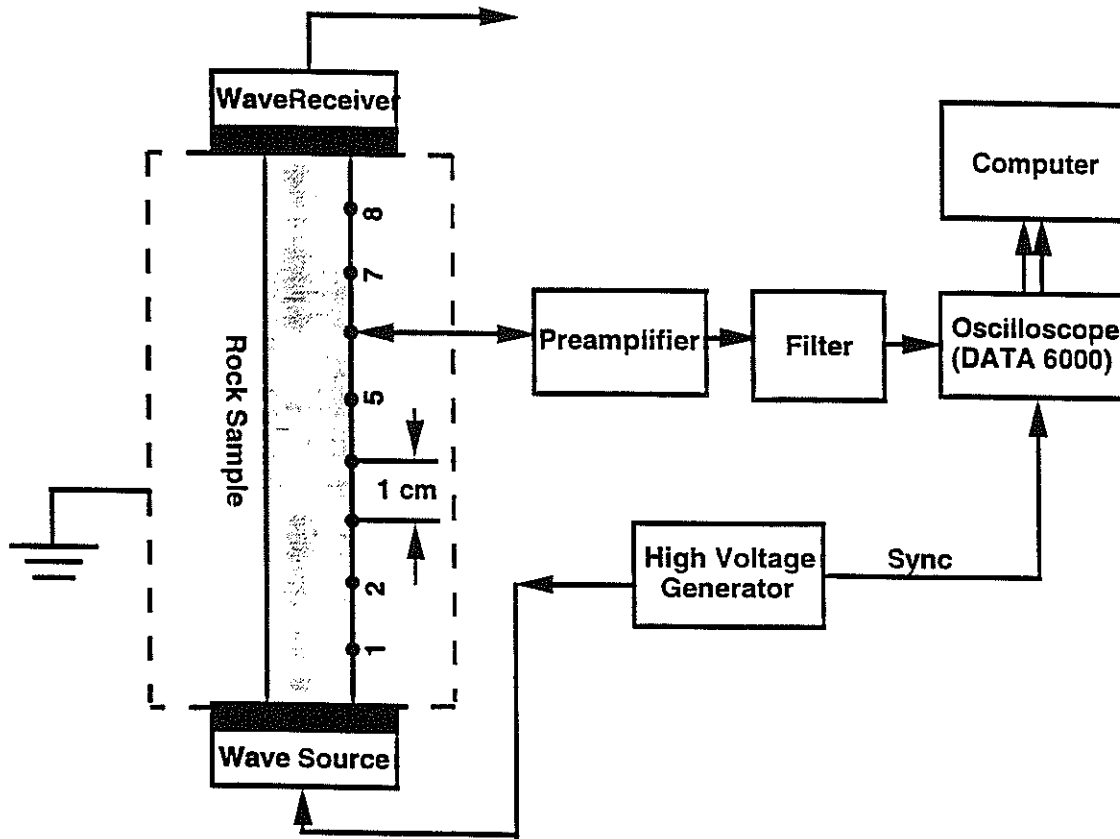
Figure 1: Experimental diagram for measuring the electric field generated by a transducer in a cylinder rock sample.
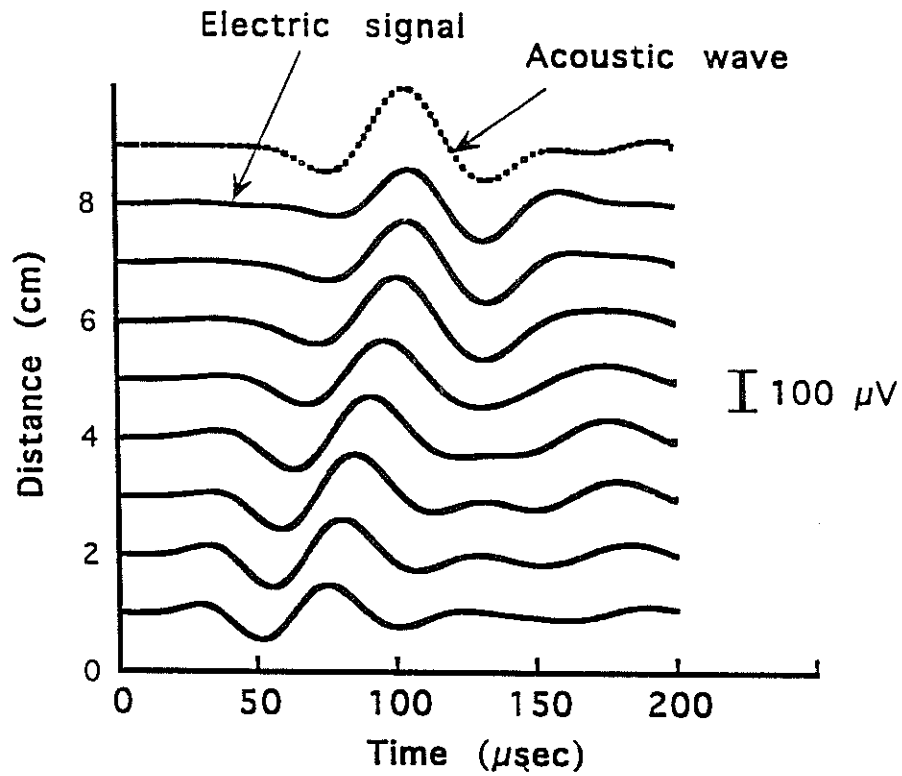
Figure 2: Electric signals generated by a P-wave transducer in a water-saturated Berea sandstone cylinder sample and the compressional wave (dotted line) received on the other end of the cylinder.

Electric signal   Acoustic wave
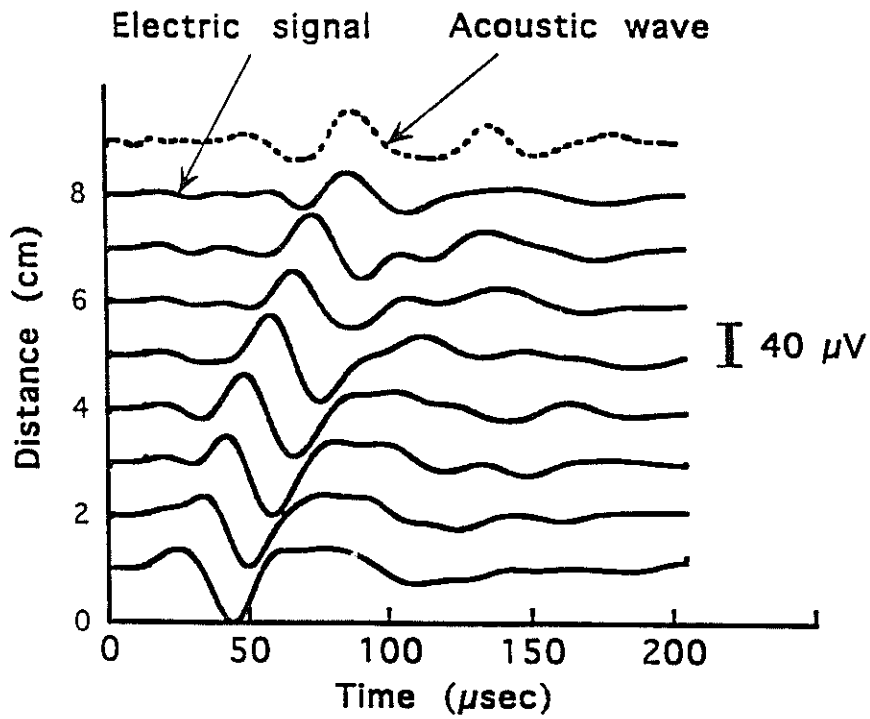
Figure 3: Electric signals generated by an S-wave transducer in a water-saturated Coconino sandstone cylinder sample and the shear wave (dotted line) received on the other end of the cylinder.

P-wave Source
(fo= 100 kHz)

45°

Lucite

11 cm

8 cm

2 cm

1 2 3 4 5 6 9 10

2.4cm

Rock sample

25 cm
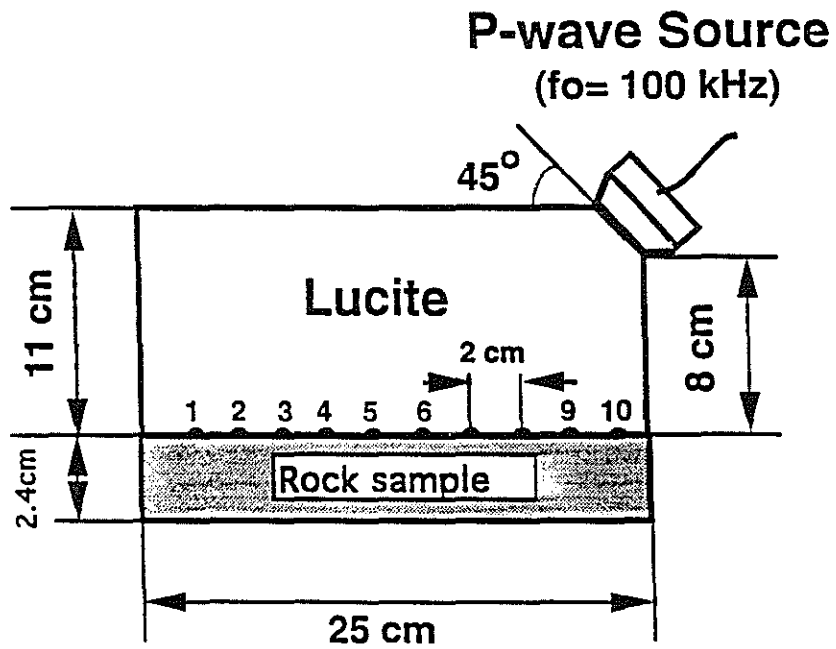
Figure 4: A layer model for measuring the electric signals generated by a P-wave at the interface between a Lucite block and a piece of sandstone.

receiver position
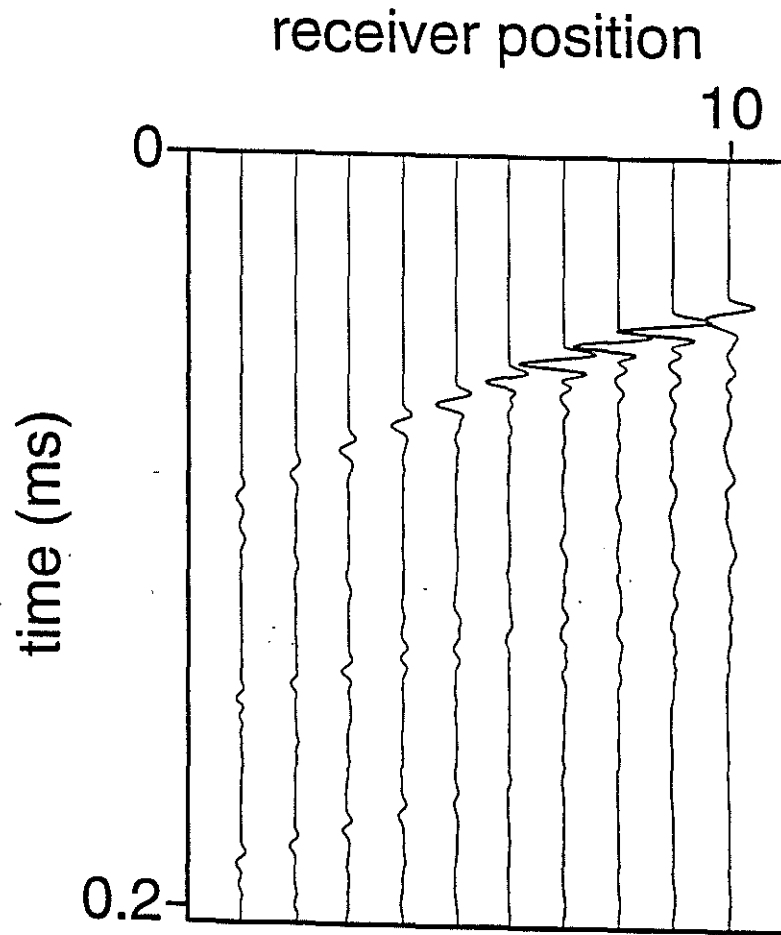
Figure 5: Normalized acoustic waveforms received by a P-wave transducer on the bottom surface of the Lucite block (Figure 4).

receiver position
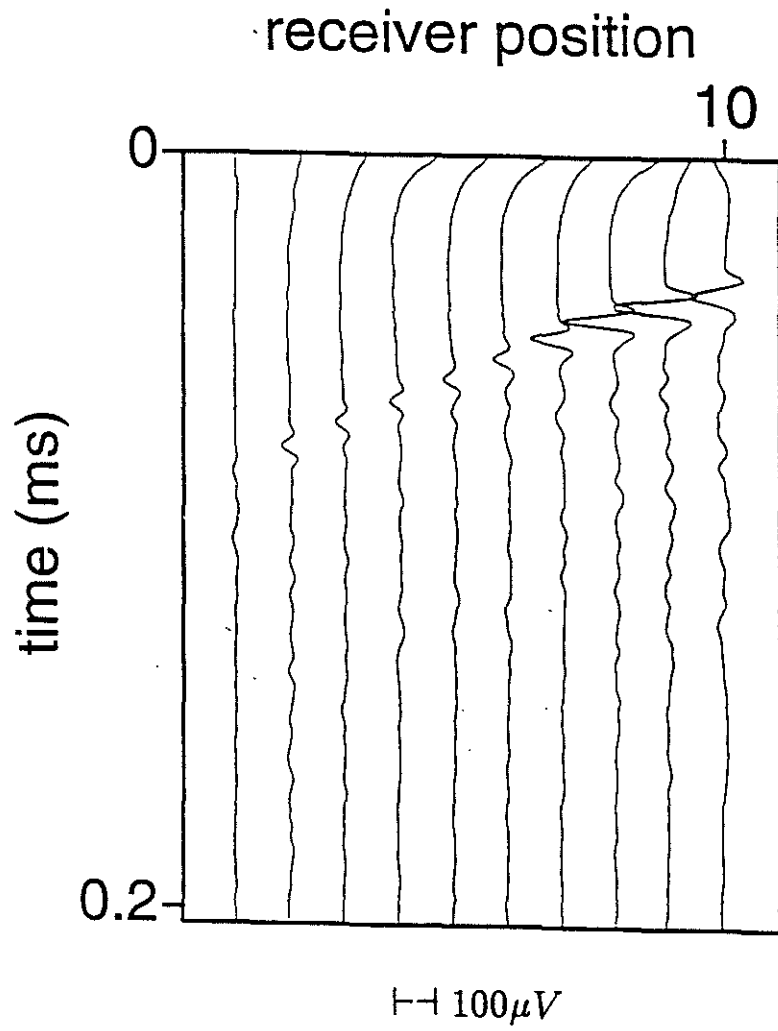
Figure 6: Electric signals received at 10 measurement points on the interface between the Lucite block and the water-saturated Berea sandstone sample.

receiver position

0

10

time (ms)

0.2

⊢⊣ $10\mu V$
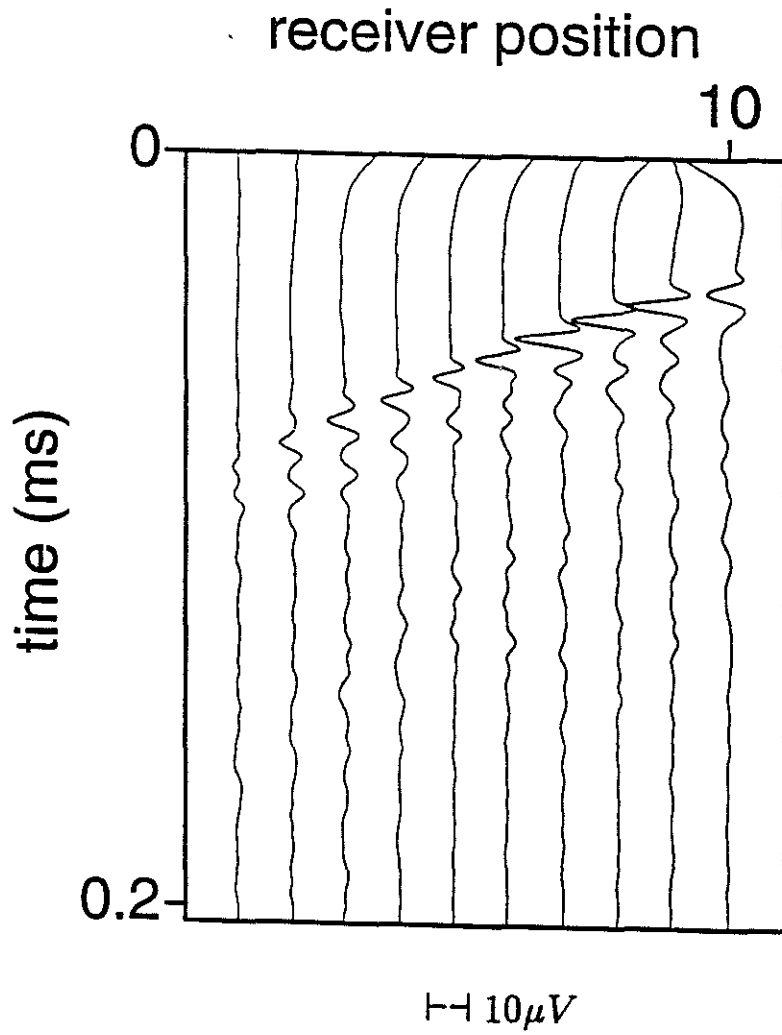
Figure 7: Electric signals received at 10 measurement points on the interface between the Lucite block and the water-saturated Coconino sandstone sample.
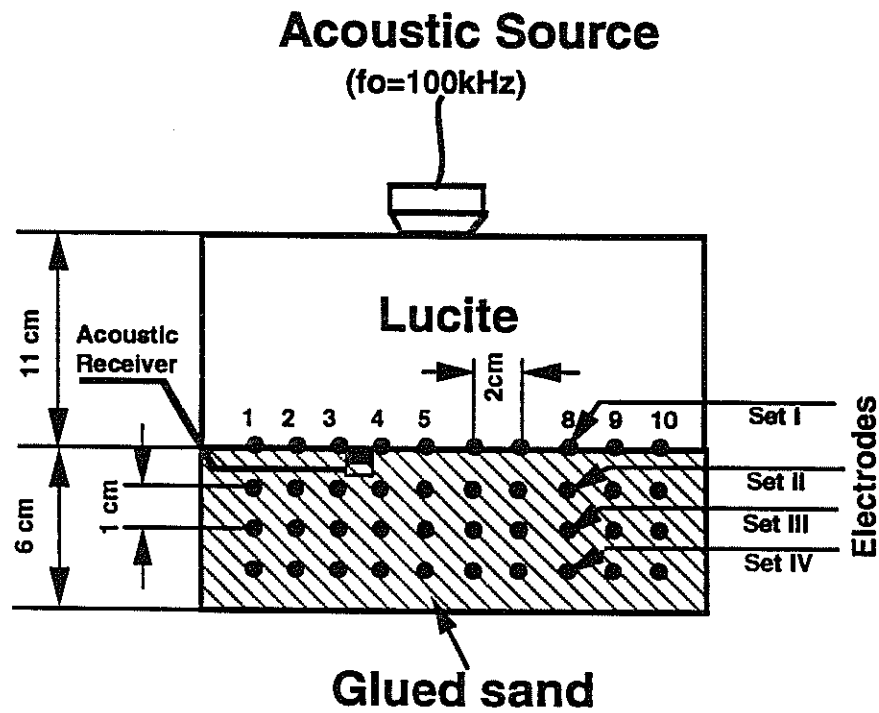
Figure 8: Man-made layer model for measuring electric signals. The parameters of the glued sand as shown in Table 1. Four sets of the electrodes are buried in the sand. The conductivity and the permeability of the water-saturated glued sand is about $280\Omega \cdot m$ and 200 darcy, respectively.
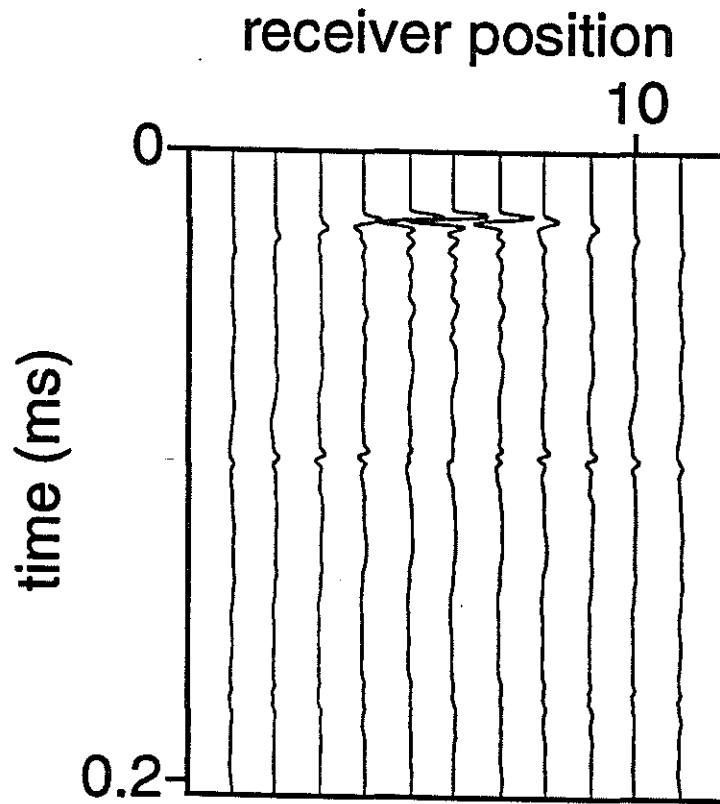
Figure 9: Normalized compressional waveforms generated by a P-wave source and received by a P-wave receiver on the bottom surface of the Lucite block (Figure 8).
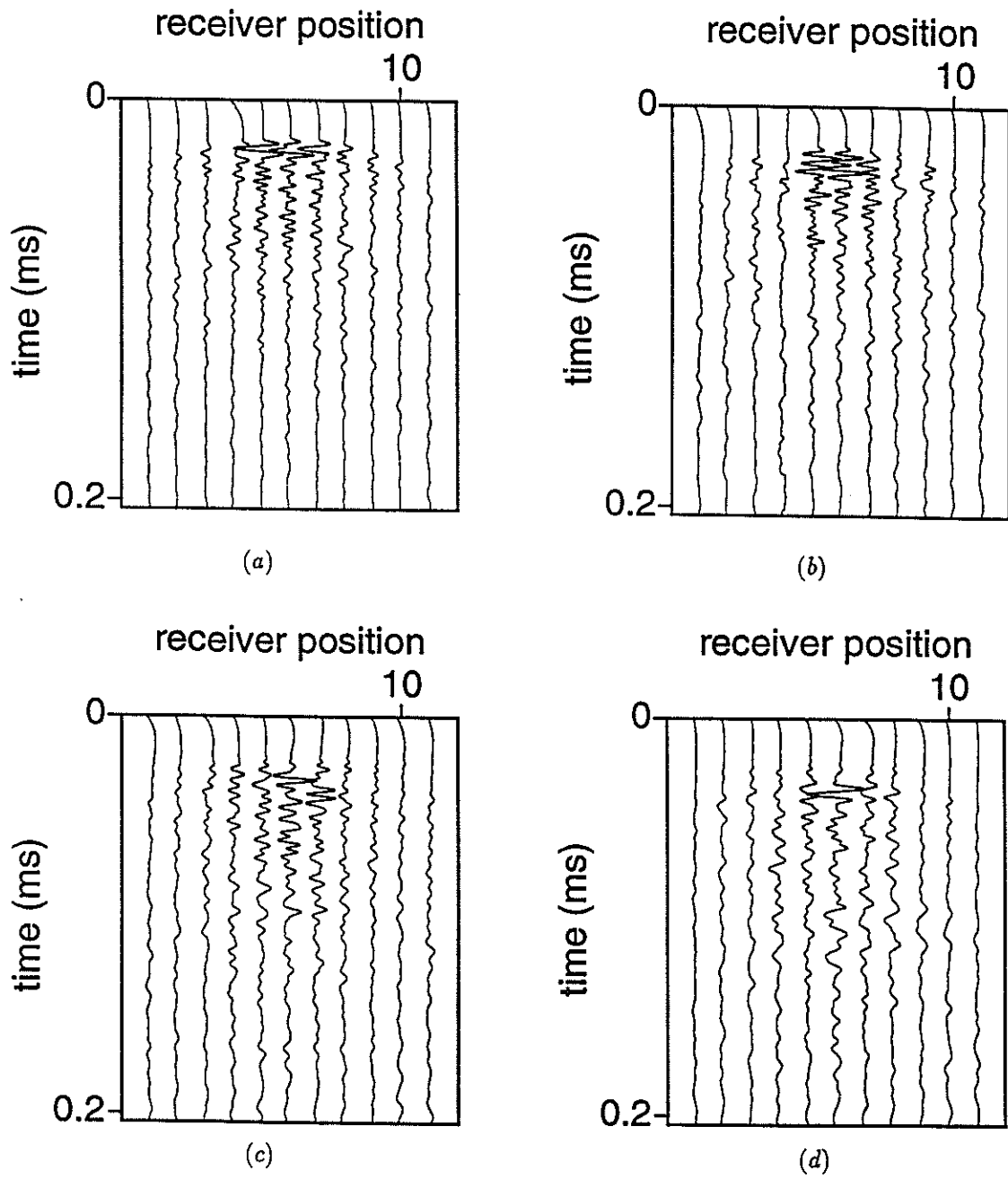
Figure 10: Electric signals generated by a P-wave source (Figure 8) and received by the electrode sets I (a), II (b), III (c), and IV (d). The amplitude is normalized by the maximum of 11 traces in each plot.
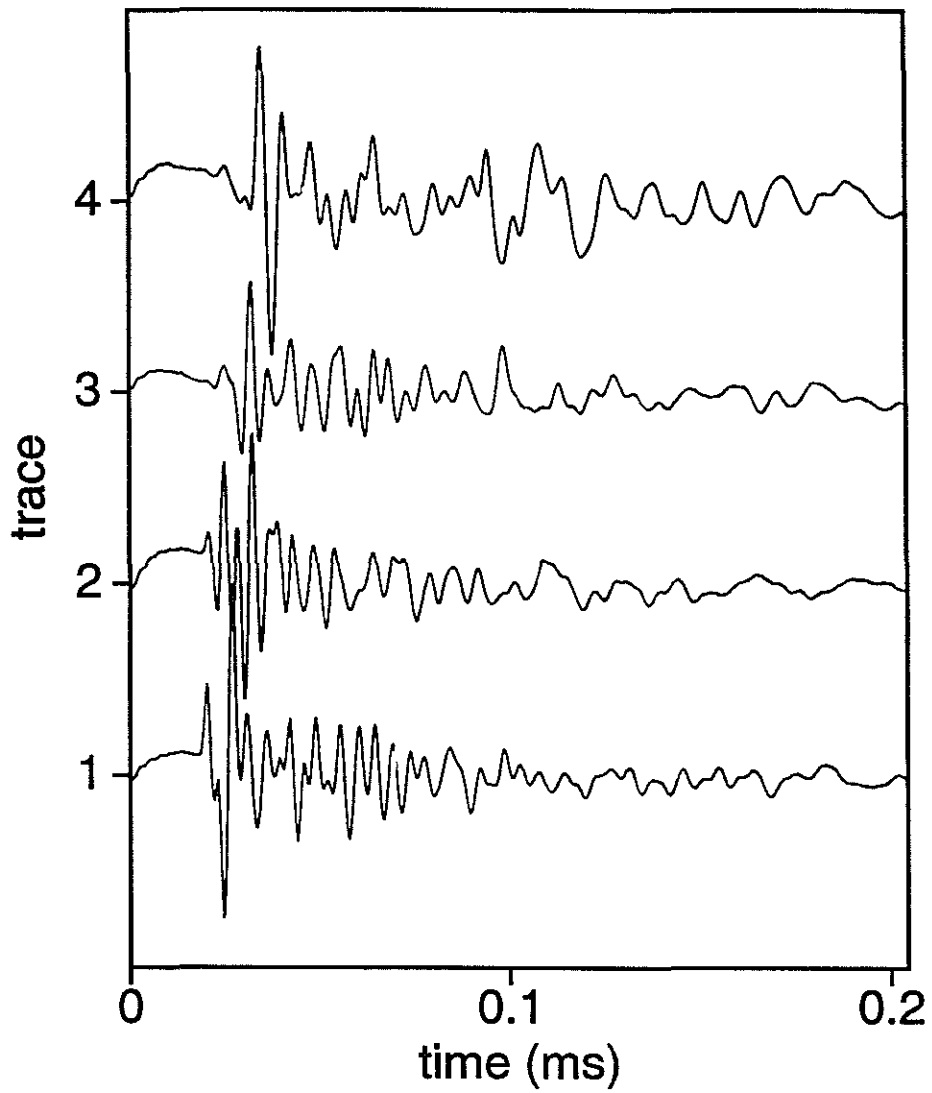
Figure 11: Electric signals received by the electrodes at the same position but different depth. The distance of the electrodes from the interface is 0 cm, 1 cm, 2 cm, and 3 cm for trace 1 to trace 4, respectively.
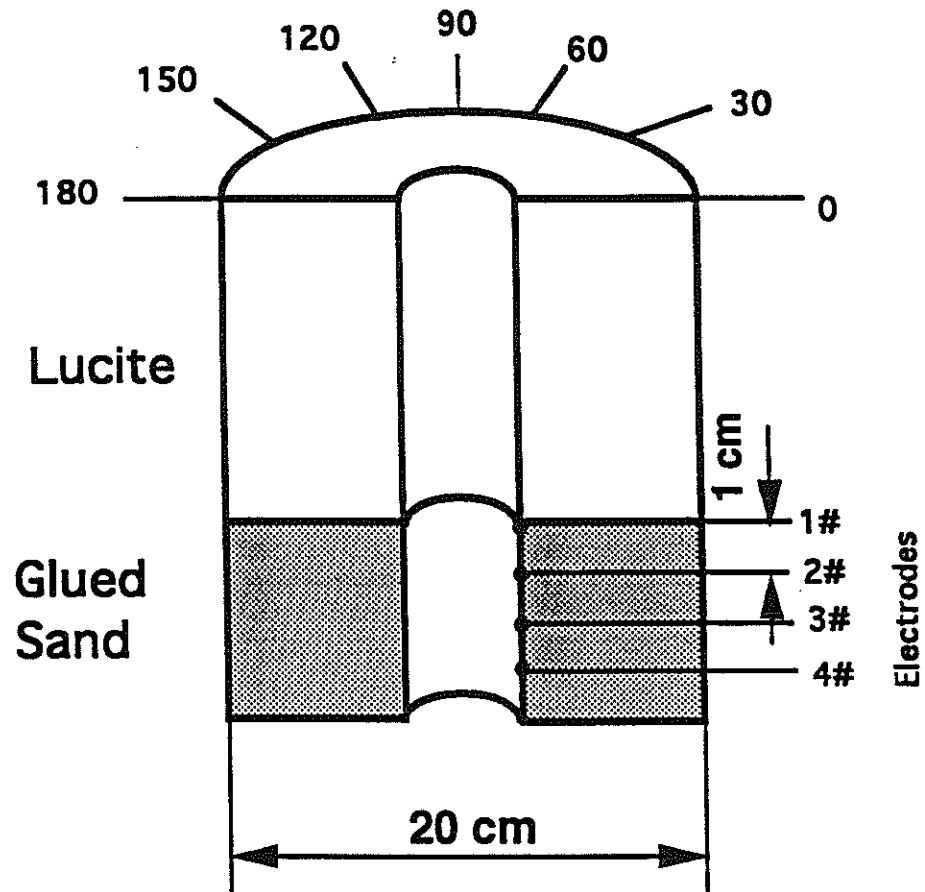
Figure 12: A borehole model made of Lucite and glued sand. The diameter of the borehole is 1.27 cm.
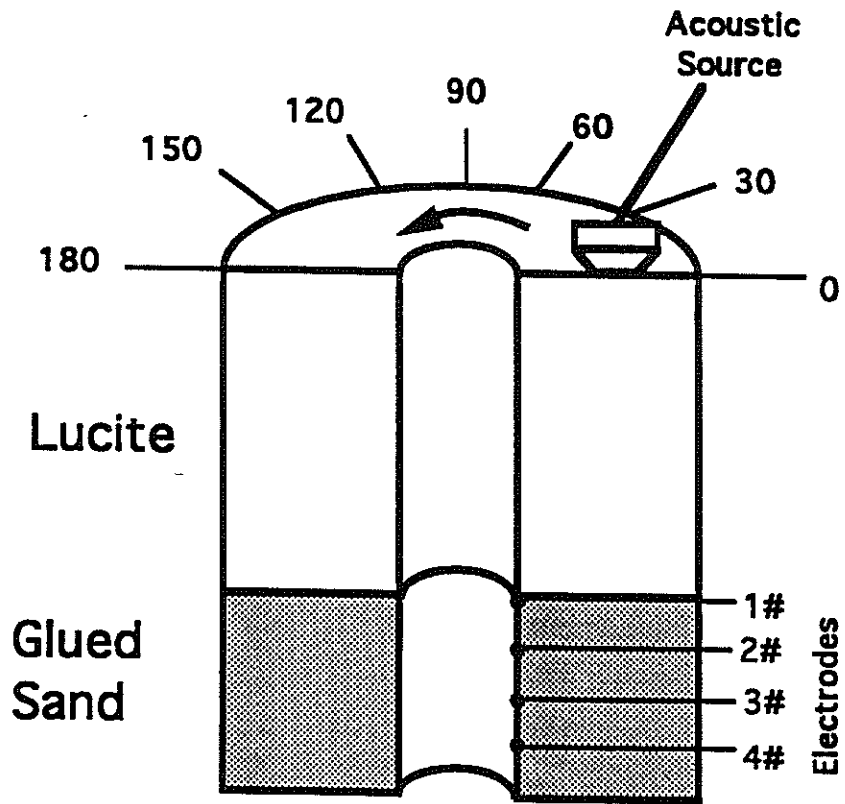
Figure 13: A diagram for VSP measurement. A compressional transducer moves around the borehole on the top side of the Lucite. The electrodes are buried in the borehole wall to receive the electric signals.
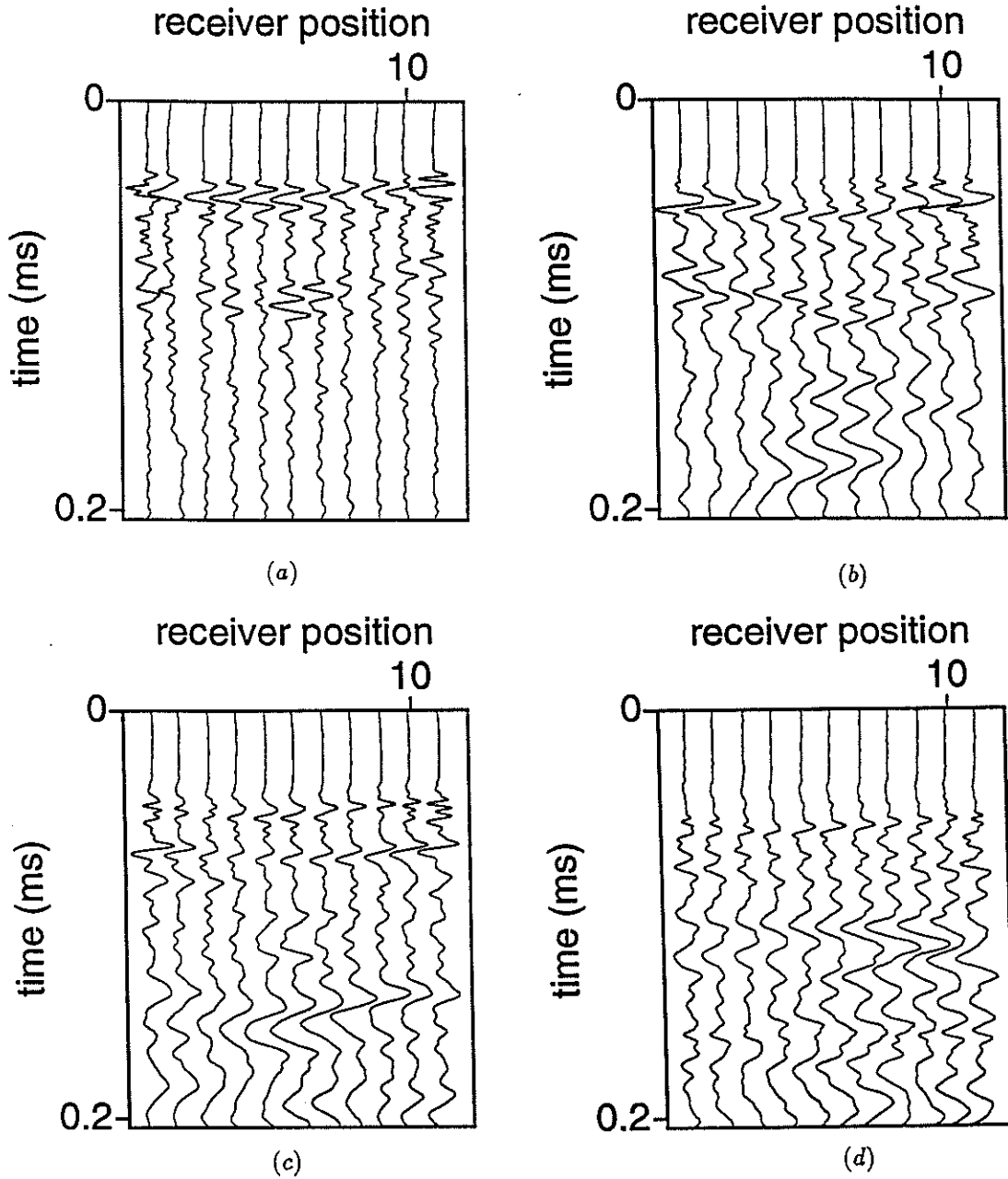
Figure 14: Electric signals received by electrodes #1 (a), #2 (b), #3 (c), and #4 (d) when the P-wave transducer moves around with 30°/trace on the top side of the Lucite. The amplitude is normalized by the maximum of 13 traces in each plot.
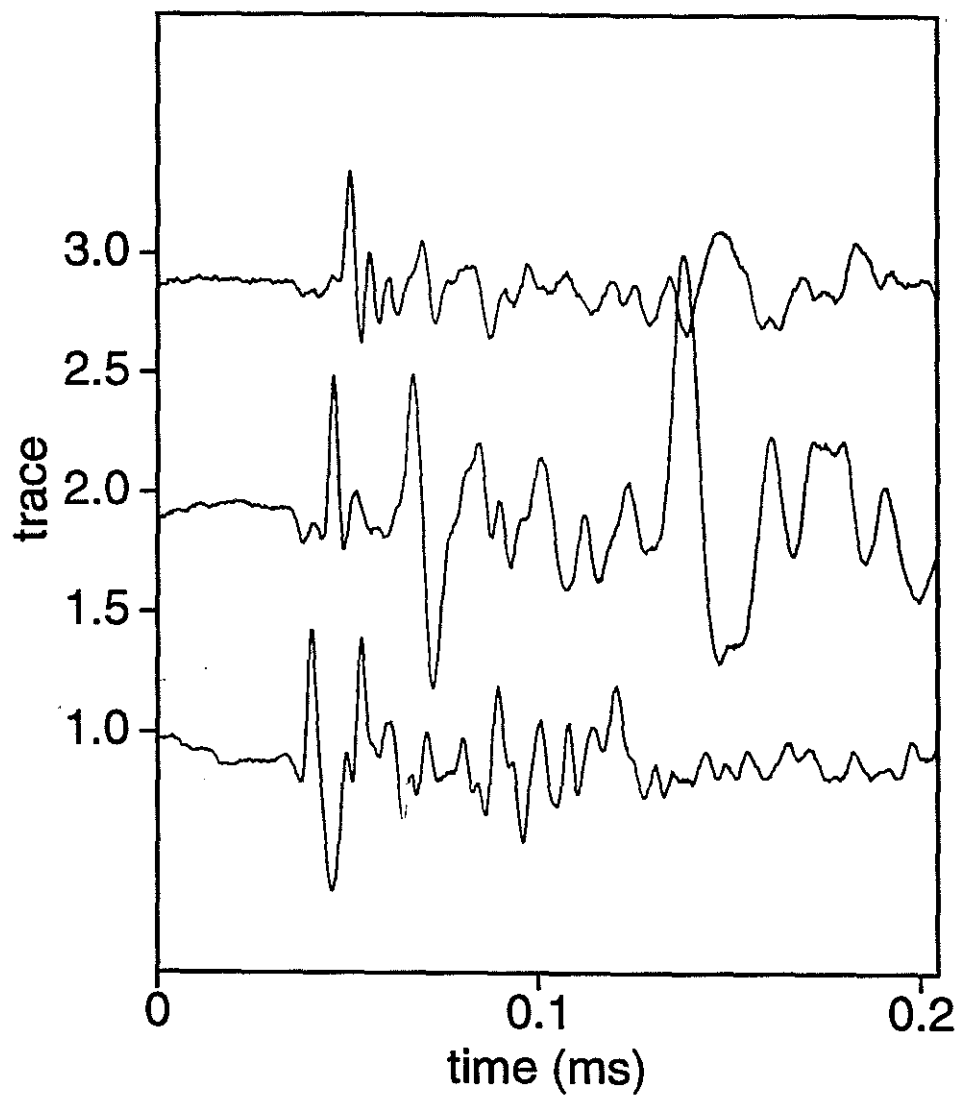
Figure 15: Electric signals received by electrodes #2, #3, and #4 when the transducer is fixed at 270°on the top side of the Lucite.
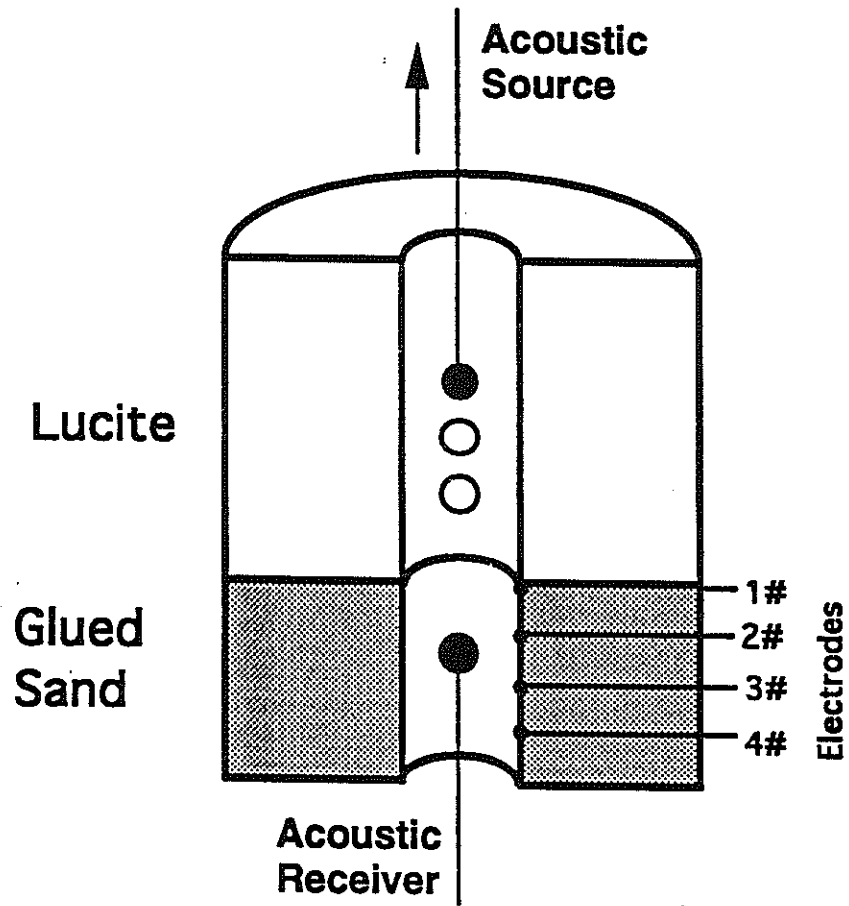
Figure 16: A diagram for borehole measurement. When an acoustic source moves up in the water-filled borehole with 1 cm spacing, the acoustic wave in the borehole and the electric signal on the borehole wall can be received and recorded by a fixed acoustic receiver and the electrodes, respectively.
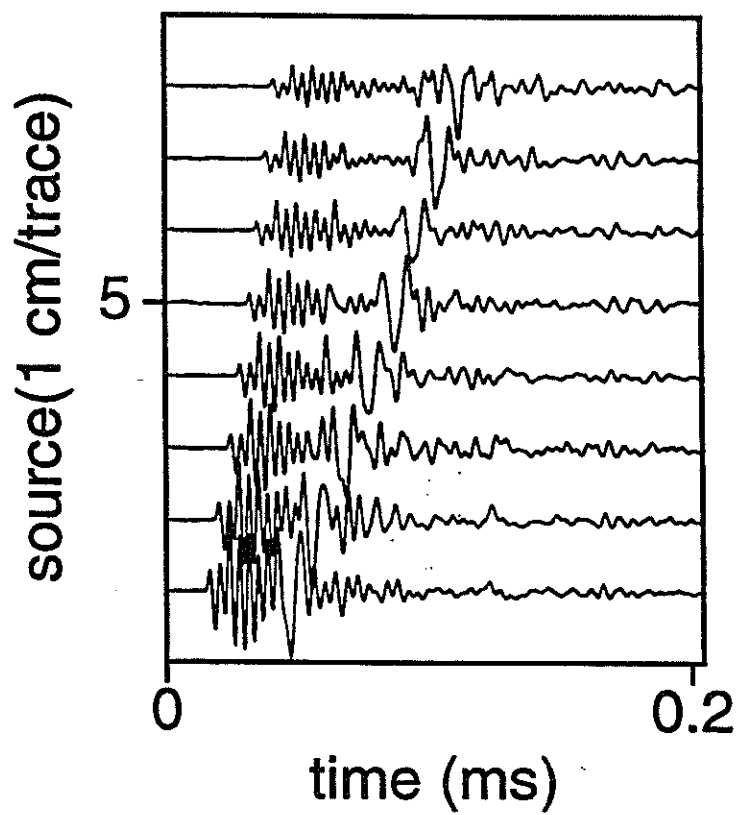
Figure 17: Acoustic wave received by an acoustic receiver fixed in the borehole section of the glued sand when the acoustic source moves up with 1 cm/trace along the water-filled borehole.
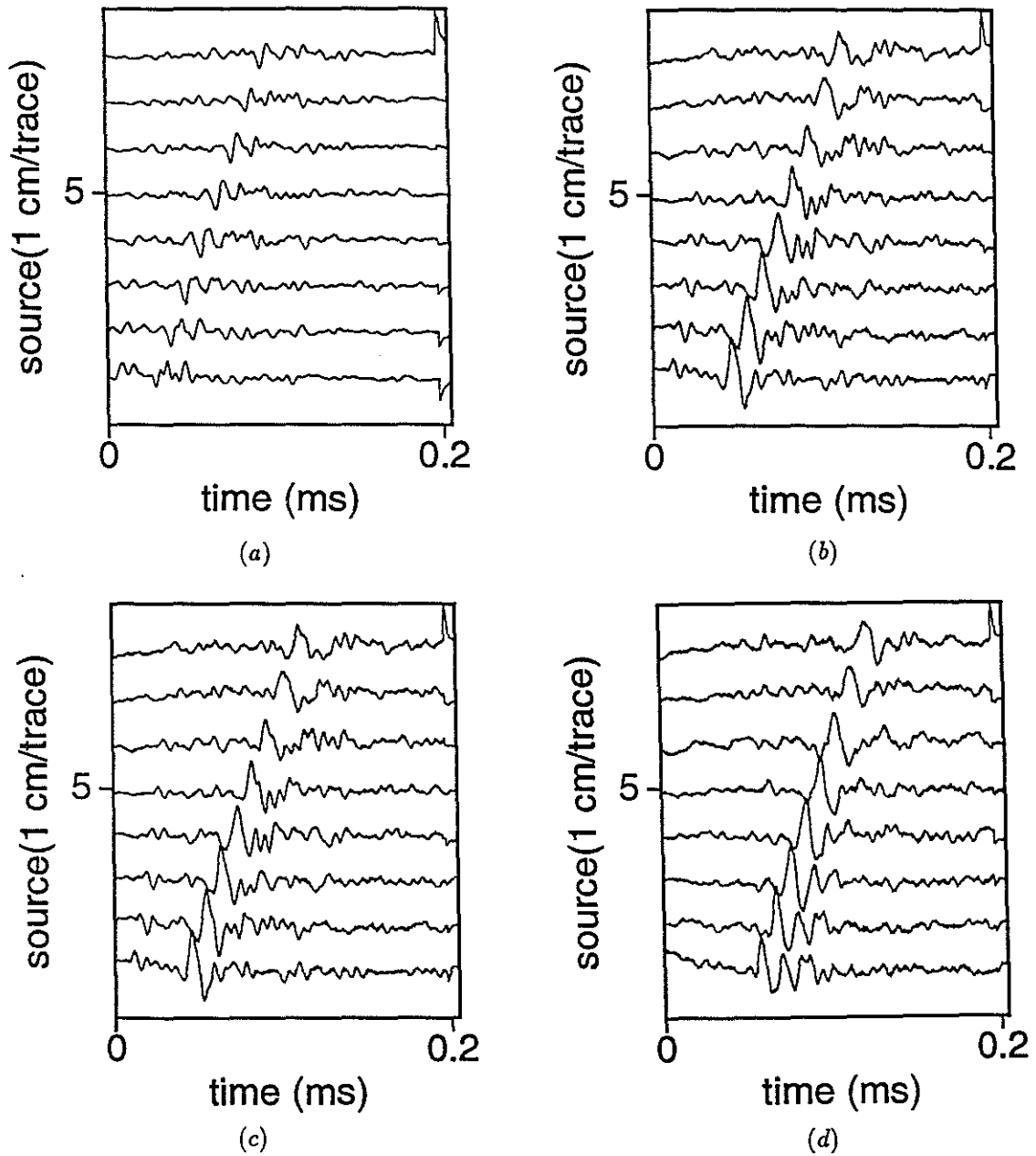
Figure 18: Electric signals received by electrodes #1 (a), #2 (b), #3 (c), and #4 (d) when the acoustic source moves up with 1 cm/trace along the water-filled borehole. The amplitude is normalized by the maximum of 8 traces in each plot.
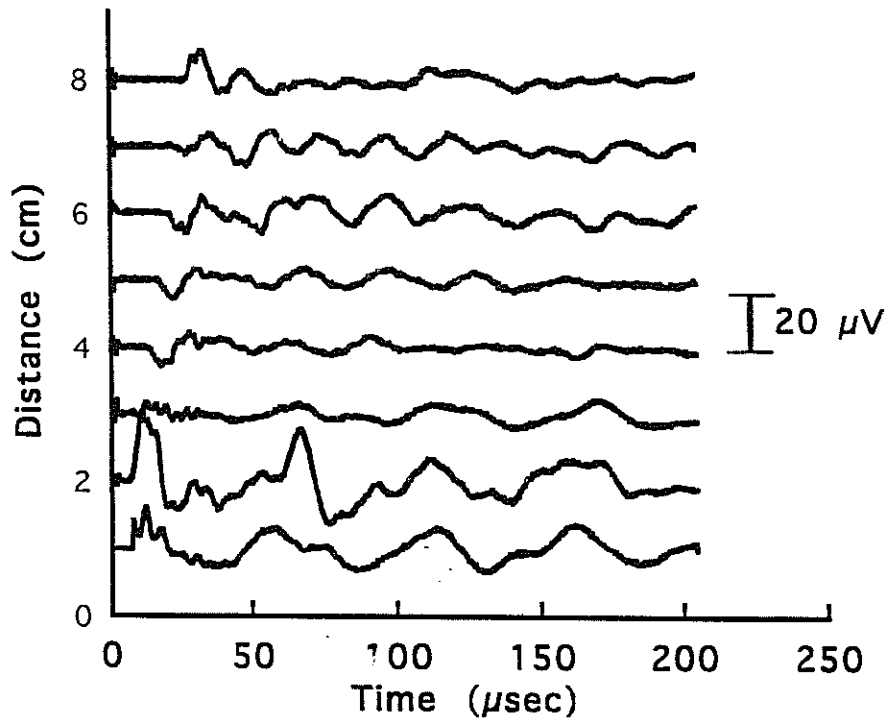
Figure 19: Electric signals generated by a P-wave transducer with a dry Berea cylinder
sample (Figure 1).